Optimal Scheduling of Integrated Energy Systems With Multiple CCHPs for High Efficiency and Low Emissions

Haimin Xie, Hui Liu, *Senior Member, IEEE*, Can Wan, *Senior Member, IEEE*, Hui Hwang Goh, *Senior Member, IEEE*, and Saifur Rahman, *Life Fellow, IEEE*

***Abstract*—In order to reach carbon neutrality, there is growing interest in reducing greenhouse gas (GHG) and improving energy efficiency. One way to address this issue is the optimal scheduling of the integrated energy system (IES) with multiple combined cooling heating and power (CCHP) systems as proposed in this article. We model IES as a device with multiple input/output ports by the energy hub (EH) framework and propose a multiobjective optimal model to improve energy efficiency and reduce GHG emissions. The proposed model is constructed as a mixed-integer nonlinear programming (MINLP) due to considering nonlinear couplings of multiple energy flows and the unit commitment of multiple CCHP systems. To improve the computational efficiency, the proposed MINLP model is transformed into a nonlinear programming (NLP) model by a fast unit commitment technique based on the approximation of the aggregated online capacity. Finally, simulation results show the effectiveness of the proposed approach in reducing GHG emissions and improving energy efficiency as well as computational efficiency.**

***Index Terms*—Combined cooling heating and power (CCHP), energy hub (EH), integrated energy system (IES), mixed-integer nonlinear programming (MINLP), optimal scheduling.**

NOMENCLATURE

Indices

t	Time.
i	Gas turbine number.
j	Electric vehicle number.
PV	Photovoltaic.
CCHP	Combined cooling heating and power.
EC	Electric chiller.
AC	Absorption chiller.
GB	Gas boiler.
EV	Electric vehicle.
TES	Thermal energy storage.

Parameters

ρ	Converting factor of 1 kWh to m^3 natural gas.
Δt	Dispatch time interval (h).
a_i, b_i, c_i	Efficiency coefficients of the GT.
α_i, β_i, γ_i	Emission coefficients of the GT (kg/MWh).
$\eta_{h,i}$	Thermal efficiency of ith CCHP.
η_{PV}	PV efficiency.
S	Size of PV (m^2).
I	Solar irradiance.
T_{out}	Ambient temperature (°C).
μ	Energy loss coefficient.
η_{in}, η_{dr}	Injecting/drawing heat efficiencies of TES.
$P_{\mathrm{in}}^{\max}$, $P_{dr}^{\max}$	Maximum inject/draw thermal of TES (MW).
$\eta_{ch,j}$, $\eta_{dch,j}$	Charge/ discharge efficiencies of jth EV.
cap_j	Battery capacity of jth EV (MWh).
$P_{ch,j}^{\max}$, $P_{dch,j}^{\max}$	Maximum charging /discharging power (MW).
$EV_j^{\max}$, $EV_j^{\min}$	Upper/lower capacity of jth EV battery.
η_{GB}	GB efficiency.
$c_{\mathrm{cs},i}$, $c_{\mathrm{cd},i}$	Start-up and shut-down offer cost of ith GT (¥).
$c_e(t)$, $c_g(t)$	Electricity and natural gas price at time t (¥).
$\varsigma_e(t)$	Extra bonus at time t (¥).
$\mathrm{cop}_{\mathrm{EC}}$	Cooling coefficient for electric chiller.
$\mathrm{cop}_{\mathrm{AC}}$	Cooling coefficient for adsorption chiller.
μ_{pc}	Emission factors of network electricity (kg/MWh).
μ_{gc}	Emission factors of natural gas (kg/m^3).
P_{CCHP}^{u}, P_{CCHP}^{d}	Ramping up/down rate of CCHP (MW/min).
UT_i, DT_i	Minimum up/ down time.
$P_{\mathrm{CCHP}}^{\max}$, $P_{\mathrm{CCHP}}^{\min}$	Maximum and minimum power of CCHP (MW).
$H_{\mathrm{GB}}^{\max}$, $H_{\mathrm{GB}}^{\min}$	Maximum/minimum thermal power of GB (MW).

Manuscript received 4 October 2022; revised 10 April 2023 and 3 July 2023; accepted 8 August 2023. Date of publication 14 August 2023; date of current version 7 December 2023. This work was supported in part by the National Key Research and Development Program of China under Grant 2019YFE0118000; in part by the National Natural Science Foundation of China under Grant 61963003; and in part by the Natural Science Foundation for Distinguished Young Scholars of Guangxi under Grant 2018GXNSFFA281006. *(Corresponding author: Hui Liu.)*

Haimin Xie, Hui Liu, and Hui Hwang Goh are with the School of Electrical Engineering, Guangxi University, Nanning 530004, China (e-mail: xhm2230@163.com; hughlh@126.com; hhgoh@gxu.edu.cn).

Can Wan is with the College of Electrical Engineering, Zhejiang University, Hangzhou 310027, China (e-mail: canwan@zju.edu.cn).

Saifur Rahman is with the Advanced Research Institute, Virginia Tech, Arlington, VA 22203 USA (e-mail: srahman@vt.edu).

Digital Object Identifier 10.1109/JIOT.2023.3304644

H^{u}_{GB}, H^{d}_{GB}	Ramping up/down rate of GB (MW/min).
$H^{\max}_{\mathrm{AC}}$, $H^{\min}_{\mathrm{AC}}$	Maximum /minimum thermal power of AC (MW).
$P^{\max}_{\mathrm{EC}}$, $P^{\min}_{\mathrm{EC}}$	Maximum/minimum electrical power of EC (MW).
$F^{\max}_{\mathrm{net}}$	Maximum natural gas bought from network (m^3).
$P^{\max}_{\mathrm{net}}$, $P^{\max}_{\mathrm{out}}$	Maximum power bought to /sold from grid (MW).
$L_e(t)$, $L_h(t)$, $L_c(t)$	Electricity, heating, and cooling load at time t (MW).

Variables

F^{C}, F^{M}	Total operation cost and GHG emissions.
$P^{\mathrm{net}}_{e}(t)$, $P^{\mathrm{out}}(t)$	Power purchased from/sold to grid (MW).
$P_{\mathrm{CCHP},i}(t)$	Power generated by the ith CCHP at time t (MW).
$\eta_{e,i}(t)$	Power efficiency of the ith CCHP at time t.
$P_{\mathrm{PV}}(t)$	Power of PV at time t (MW).
$P^{ch}_{\mathrm{EV},j}(t)$	Charing power of the jth EV at time t (MW).
$P^{dch}_{\mathrm{EV},j}(t)$	Discharging power of the jth EV at time t (MW).
$C_{\mathrm{EC}}(t)$	Cooling generated by EC at time t (MW).
$P_{\mathrm{EC}}(t)$	Required power of EC at time t (MW).
$F_{\mathrm{CCHP},i}(t)$	Fuel consumption of CCHP at time t (m^3).
$F_{\mathrm{GB}}(t)$	Fuel consumption of GB at time t (m^3).
$H_{\mathrm{CCHP},i}(t)$	Heat generated by ith CCHP at time t (MW).
$H_{\mathrm{GB}}(t)$	Heat generated by GB at time t (MW).
$C_{\mathrm{AC}}(t)$	Cooling generated by AC at time t (MW).
$H_{\mathrm{AC}}(t)$	Required heating of AC at time t (MW).
$H^{\mathrm{in}}_{\mathrm{TES}}(t)$, $H^{dr}_{\mathrm{TES}}(t)$	Inject and draw heat of TES at time t (MW).
$Q_{\mathrm{TES}}(t)$	Heat stored in TES at time t (MWh).

Binary Variables

$v_i(t)$	On/off status of the ith CCHP at time t.
$y_i(t)$, $z_i(t)$	Start up and shut down status of the ith CCHP at time t.

I. Introduction

THE CRISIS of fossil fuel energy and greenhouse gas (GHG) emissions has become a considerable concern around the world. The traditional energy management mode in which energy systems are planned and operated independently exacerbates this situation [1]. To deal with this crisis, the concept of the integrated energy system (IES) is proposed as a promising solution [2], [3]. This is because IESs can incorporate renewable energy, energy conversion devices (cooling heating and power (CCHP) systems, heating boiler, etc.), energy storage facilities (electrical/thermal/gas storage energy, etc.), and flexible resources (electric vehicles, air conditioners, etc.) to realize efficient and low-carbon utilization [4].

As the most important subsystem of IES, some optimal operation strategies are proposed to explore the performance of CCHP. One of the most common operation strategies is the cost-oriented strategy. For instance, a minimum distance operation strategy is proposed to maintain the high efficiency of the CCHP [5]. A techno-economic optimal model is developed to maximize the economic benefit [6]. Besides, considering different scenarios, the economics of CCHPs in office buildings, hotels, and hospitals could be improved through the "Smart" operation strategy [7]. Because of the global concern about the climate change, considering GHG emissions has also gained a lot of interest in analyzing energy systems. Therefore, an emission operation strategy is proposed to minimize the GHG emissions from CCHPs [8]. The result shows that lower GHG emissions can be achieved, compared to the strategy only aiming at reducing primary energy consumption. Subsequently, the primary energy consumption, operation cost, and GHG emissions are separately evaluated by an optimal operation scheme of CCHPs under different climate conditions [9]. Comparatively, multiobjective optimization models for CCHP are proposed in [10] and [11] to simultaneously minimize primary energy consumption, operation cost, and GHG emissions, which is capable of effectively balancing the influences of consumption, cost, and emissions. The objectives of the optimal strategies mentioned above are to optimize the output of an individual CCHP for electricity, heating, and cooling. However, with modern energy conversion technologies, the interaction between multienergy systems becomes more complex.

The energy hub (EH) concept first proposed in [12], is used as a framework for multienergy systems to describe the coupling and collaboration of different energy flows. Therefore, the optimal operation of the EH with the CCHP has been recognized to reduce operation cost [13], [14], [15], [16], [17], [18], [19], [20], [21], [22], [23] and GHG emissions [20], [21], [22], [23] from energy storages, uncertain renewable resources, and demand responses, respectively, as shown in Table I. Ha et al. [13], Yang et al. [14], and Heidari [15] discussed the effect of energy storage systems on the EH operation cost. In [13], an optimal model of the EH with CCHP is proposed to analyze the impact of electrical storage energy on economic improvement. The effect of thermal energy storage on the performance and economic benefit of EH is investigated in [14], while the ice storage system is studied in [15]. It is shown that the thermal/ice storage can increase the flexibility of EH in integrating energy resources, thereby reducing energy purchasing cost. The wind power uncertainty is discussed in [16] and [17]. A stochastic programming model is developed for the EH with CCHP to minimize the total operation cost [16], while a robust chance-constrained optimization framework is proposed to discuss the optimal operation of an EH [17]. Besides, demand response is proven can reduce the energy purchasing cost of EH with CCHP [18]. Subsequently, by utilizing the price-based demand response, a coordinated operation of EH with CCHP is proposed to minimize the total operation cost [19]. However, in [13], [14], [15], [16], [17], [18], and [19], the optimal models are only discussed from the perspective of economic cost. As shown in [20], [21], [22],

TABLE I
LIST OF SOME STUDIES ON OPTIMAL OPERATION OF EH WITH CCHP

Ref.	EH structures				Nonlinear coupling of CCHP power efficiency and GHG emissions	Objective	Model
	converters	storage	uncertainty	DR			
[13]	S-CCHP	ESS	×	×	×	Min. total energy purchasing cost	SO
[14]	S-CCHP, RES, GB, HE, AC, EC	TES	×	√	×	Min. total operation cost	SO
[15]	S-CCHP, RES	ESS, TES, ISS	√	√	×	Min. total energy purchasing cost	SO
[16]	S-CCHP, EHP, RES	×	√	×	×	Min. total operation cost	SO
[17]	CCHP, EHP, GB,	ESS	√	×	×	Min. total operation cost	SO
[18]	S-CCHP, EHe, AC, EC, GF	TES, ESS	×	√	×	Min. total energy purchasing cost	SO
[19]	S-CCHP, RES, HC	TES	√	√	×	Min. total operation cost	SO
[20]	S-CCHP, RES, GB, HE, AC, EC	TES, ISS, ESS	×	√	×	Min. total energy purchasing and emissions costs	SO
[21]	S-CCHP, RES, AC, EHe	ESS, ISS, TES	×	×	×	Min. total energy purchasing and emissions costs	SO
[22]	S-CCHP, GT, GF, HRB, AC, EC	ESS, TSS	×	√	×	Min. total operation and emissions costs	SO
[23]	S-CCHP, AC, EC, RES	ESS, TES	×	√	×	Min. total energy purchasing and emissions costs	MO
Proposed model	**Multi-CCHPs, RES, EC, AC, GB,**	**ESS, TES**	×	×	√	**Min. total operation and emissions costs**	**MO**

DR for demand response; S-CCHP for single CCHP; Multi-CCHP for multiple CCHPs; RES for renewable energy resources; HE for heating exchanger; EHP for Electric Heat Pump; GT for gas turbine; GF for gas furnace; EHe for electric heater; HC for Heating coil; HRB for heat recovery boiler; ESS for electrical storage system; ISS for ice storage system; SO for single-objective optimization; MO for multi-objective optimization. *①The total operation cost includes energy purchasing cost, energy selling revenue, startup/shutdown cost, etc. ② √ means that the item is considered, otherwise × is used.

and [23], the environment also has a significant influence on the optimal operation of EH with CCHP. In [20] and [21], an optimal scheduling model is proposed to reduce the total energy purchasing and GHG emissions cost. In [22], considering the influence of the pollutant trading market on total operation cost, an optimal scheduling strategy is proposed to minimize the operation and emission cost of the EH. While considering the environmental influence cost, a single-objective model is constructed in [20], [21], and [22]. This formulation, however, results in a difficulty in coordinating the operation cost and GHG emission. Therefore, a multiobjective model for the EH with CCHP is proposed in [23]. As the efficiency and emissions coefficients of CCHP are considered as constants, the influence of the load rate on the power efficiency and GHG emissions is ignored, although it can play an important role in coordinating the operation cost and GHG emission. Note that the researches in [13], [14], [15], [16], [17], [18], [19], [20], [21], [22], and [23] mainly focus on the optimal scheduling of the IES with a single CCHP. The commitment operation of multiple CCHPs with different capacities, which can significantly reduce GHG emissions and improve energy efficiency, has been missing.

On the other hand, the optimal operation of IES with CCHP is modeled as a mixed-integer nonlinear programming (MINLP) problem while considering storage energy systems, nonlinear objective functions, etc. It is hard to solve the MINLP model due to a computationally intensive NP-hard model. Therefore, the model is usually transformed into mixed-integer linear programming (MILP) [24], [25] or nonlinear programming (NLP) [26]. For example, in [24], the optimal model of IES with CCHP and wind power is modeled as a MINLP problem and transformed into a MILP problem by using a piecewise linear function. A MINLP problem is proposed to minimize the total operation cost [25], in which the model is transformed into a MILP problem by a linear computation process. As such formulations will not change the mix-integer nature of the problem [27], the computational burden cannot be reduced significantly. Therefore, transforming MINLP into NLP is gradually paid attention to. In [26], mixed-integer variables are considered as continuous variables by relaxing the lower limits of decision variables but leading to the loss of computational accuracy.

In this article, an optimal scheduling of the IES with multiple CCHPs is proposed and modeled as a MINLP problem to improve energy efficiency and reduce GHG emissions. Moreover, the model is constructed as a multiobjective problem to find the tradeoff between these two objectives. The notable feature of the proposed model is that multiple CCHPs with different capacities can be flexibly combined to follow different load levels. To improve the computational efficiency and simultaneously keep high-computational accuracy, the proposed MINLP model is transformed into a NLP one by a fast unit commitment technique [28]. The main contributions of this article are summarized as follow.

1) An EH framework is proposed to enable the commitment operation of multiple CCHPs with different capacities to coordinate multiple energy flows (i.e., electricity, thermal, cooling, natural gas, and emissions), while satisfying different load levels.
2) An optimal scheduling of the IES with multiple CCHPs is proposed to improve energy efficiency and reduce GHG emissions, which is modeled as a MINLP model due to considering the nonlinear coupling and unit commitment of multiple CCHPs.
3) The proposed optimal scheduling is modeled as a multiobjective model to achieve the tradeoff between the operation cost and GHG emissions, because the power efficiency and GHG emissions can be regulated according to the CCHP load rate.

4) To improve the computational efficiency and simultaneously ensure computational accuracy, the fast unit commitment technique is used to transform the proposed MINLP model into a NLP one based on the approximation of the aggregated online capacity.

The remainder of this article is organized as follows. In Section II, the scheduling problem of the IES with multiple CCHPs is proposed. The descriptions and mathematical modeling of IES are addressed in Section III. In Section IV, the optimal scheduling of the IES with multiple CCHPs is proposed and modeled as a MINLP model. In Section V, the proposed MINLP model is transformed into a NLP one by a fast commitment method. Simulation results are provided to validate the effectiveness of the proposed model in Section VI. Finally, the conclusions are drawn in Section VII.

II. Problem Descriptions

A. Efficiency and Emissions of CCHP Systems

The ability of the CCHP to significantly improve energy efficiency and reduce GHG emissions gives the potential to become a key solution for carbon neutrality. Note that the energy efficiency here specifically refers to the energy conversion efficiency. For clarity, we here discuss the nonlinear coupling between the power efficiency and GHG emissions of CCHP and its load and capacity.

The power efficiency and GHG emissions of CCHP are decided by its capacity and load rate [29], [30]. Moreover, the power efficiency can be expressed with a second-order polynomial of the load as [31], [32]

$$\eta_{e,i}(t) = a_i + b_i \cdot P_{\mathrm{CCHP},i}(t) + c_i \cdot {P_{\mathrm{CCHP},i}}^2(t) \qquad (1a)$$

where $c_i < 0$, which means that the second-order polynomial is open downward.

As for GHG emissions, an upward-opening polynomial plus an exponential term related to the CCHP output power is considered [33], [34]. Therefore, GHG emissions have a strong nonlinear with its load, accompanied by a valley value. For convenience, we use an upward-opening polynomial to describe the relationship between the GHG emissions and the load as

$$E_{\mathrm{CCHP},i}(t) = \alpha_i + \beta_i \cdot P_{\mathrm{CCHP},i}(t) + \gamma_i \cdot P^2_{\mathrm{CCHP},i}(t) \qquad (1b)$$

where $\gamma_i > 0$.

Therefore, CCHP has different power efficiencies and GHG emissions at different load levels, as shown in Figs. 1 and 2. At the low-load levels, the power efficiency increases with the load (see Points a to c in Fig. 1). Meanwhile, GHG emissions decrease (see Point a' to c' in Fig. 2). However, at the high-load levels, GHG emissions increase with the load, and the power efficiency decreases. In addition, the high-power efficiency does not imply low-GHG emissions. Therefore, an appropriate load level can effectively coordinate power efficiency and GHG emissions.

On the other hand, CCHPs with different capacities can achieve different power efficiencies and GHG emissions, as demonstrated in Figs. 1 and 2. For instance, CCHP with a higher capacity has a lower power efficiency and higher GHG emissions at a low-load level. At the high-load level, CCHP with the higher capacity has the better power efficiency and lower GHG emissions. Therefore, multiple CCHPs with different capacities can be combined to coordinate energy efficiency and GHG emissions while satisfying different load levels.

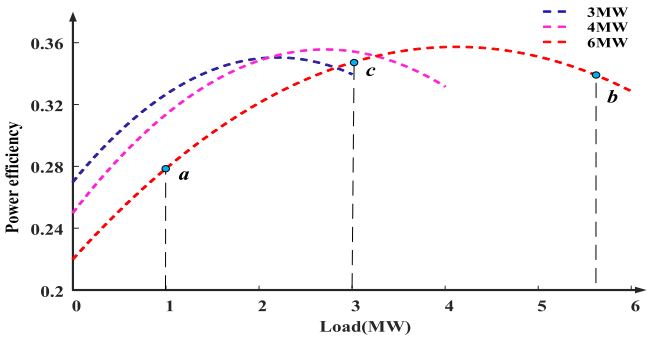

Fig. 1. Relationship between power efficiency and the load.

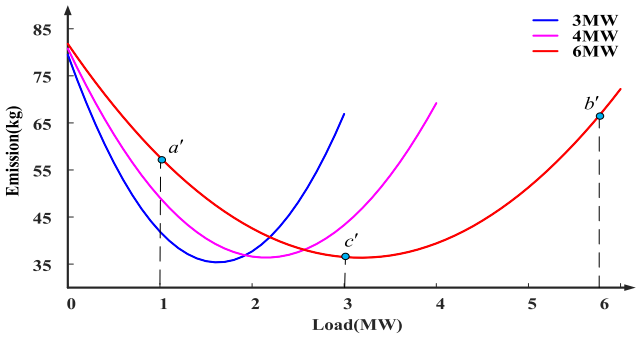

Fig. 2. Relationship between GHG emissions and the load.

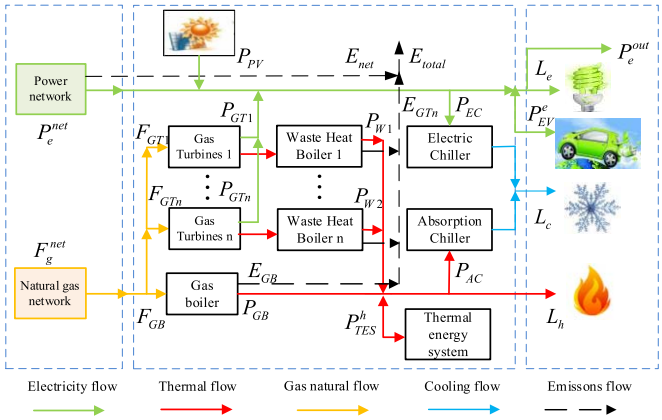

Fig. 3. Proposed framework of the EH with multiple CCHP systems.

B. Scheduling Problem of IES With Multiple CCHP Systems

As a typical application of multienergy systems, the IES on the demand side is here discussed. To achieve an effective tradeoff between energy efficiency and GHG emissions, an EH framework on multiple CCHPs with different capacities is proposed, as illustrated in Fig. 3. Note that each CCHP system consisting of a gas turbine and a waste heat boiler links the power network, natural gas network, and heating system.

Instead of using a single CCHP with a large capacity, multiple CCHPs with different capacities are here considered. This is because multiple CCHPs can be flexibly combined to

ensure high-power efficiency and low-GHG emissions, while following different load levels. For instance, in off-peak hours, CCHP with a small capacity will run to avoid the low-power efficiency and high-GHG emissions.

III. System Description and Mathematical Modeling

As shown in Fig. 3, the proposed EH framework includes CCHPs systems, thermal energy storage, photovoltaic power generation system, gas boiler, etc. Note that multiple CCHPs are the key to the proposed framework, and the power, heating, and cooling network are neglected due to the short-distance energy supply [23], [35].

A. Multiple CCHP Systems

In CCHP systems, the relationships between the generated electricity and the heating and natural gas consumption are formulated as (1c) and (1d)

$$F_{\mathrm{CCHP},i}(t) = \frac{P_{\mathrm{CCHP},i}(t)}{\eta_{e,i}(t)} \cdot \rho \cdot \Delta t \tag{1c}$$

$$H_{\mathrm{CCHP},i}(t) = F_{\mathrm{CCHP},i}(t) \cdot (1-\eta_{e,i}(t)) \frac{\eta_{h,i}}{\rho \cdot \Delta t}. \tag{1d}$$

As multiple CCHPs are considered, the mixed-integer unit commitment constraints of CCHP are considered. Typically, three binary variables are used to describe the operational status of every CCHP

$$y_i(t) - z_i(t) = v_i(t) - v_i(t-1) \tag{1e}$$

$$y_i(t) + z_i(t) \le 1 \tag{1f}$$

$$\forall i, tv_i(t), y_i(t), z_i(t) \in \{0,1\}. \tag{1g}$$

In (1e) and (1f), the binary variable $v_i(t)$ equals to 1 if the ith CCHP is on and 0 otherwise. Likewise, the start-up and shut-down status of the CCHP are shown by $y_i(t)$ and $z_i(t)$.

Therefore, the maximum and minimum output powers are constrained by (1h). Ramping constraints are expressed as (1i). Besides, (1g) or (1k) describe the minimum up/down time to avoid the frequent start/stop

$$P^{\min}_{\mathrm{CCHP},i} \cdot v_i(t) \le P_{\mathrm{CCHP},i}(t) \le P^{\max}_{\mathrm{CCHP},i} \cdot v_i(t) \tag{1h}$$

$$\begin{cases} P_{\mathrm{CCHP},i}(t) - P_{\mathrm{CCHP},i}(t-1) \le (v_i(t-1)+y_i(t)) \cdot P^{u}_{\mathrm{CCHP},i} \cdot \Delta t \\ P_{\mathrm{CCHP},i}(t) - P_{\mathrm{CCHP},i}(t-1) \ge -(v_i(t)+z_i(t)) \cdot P^{d}_{\mathrm{CCHP},i} \cdot \Delta t \end{cases} \tag{1i}$$

$$\begin{cases} \sum_{t=1}^{\xi_i} 1 - v_i(t) = 0 \\ \sum_{t=k}^{k+UT_i-1} v_i(t) \ge UT_i y_i(k) \quad \forall k = \xi_i + 1 \cdots T - UT_i + 1 \\ \sum_{t=k}^{T} v_i(t) - y_i(t) \ge 0 \quad \forall k = T - UT_i + 2 \cdots T \\ \xi_i = \min\{T, (UT_i - U_i^0) v_i(t=0)\} \end{cases} \tag{1j}$$

$$\begin{cases} \sum_{t=1}^{\zeta_i} v_i(t) = 0 \\ \sum_{t=k}^{k+DT_i-1} 1 - v_i(t) \ge DT_i z_i(k) \quad \forall k = \zeta_i + 1 \cdots T - DT_i + 1 \\ \sum_{t=k}^{T} 1 - v_i(t) - z_i(t) \ge 0 \quad \forall k = T - DT_i + 2 \cdots T \\ \zeta_i = \min\{T, (DT_i - S_i^0)(1 - v_i(t=0))\}. \end{cases} \tag{1k}$$

B. Thermal Energy System

Constraints for the thermal energy system are shown in (2). The heat variation of the thermal energy system during an interval Δt is shown by (2a). With (2b), the upper and lower limits of the thermal energy system are considered. Constraints (2c) and (2d) refer to the injecting and drawing heat during Δt. Injecting and drawing thermal energy cannot coexist by

$$Q_{\mathrm{TES}}(t) = Q_{\mathrm{TES}}(t-1) \cdot (1-\mu) + \left(\eta_{\mathrm{in}} \cdot H^{\mathrm{in}}_{\mathrm{TES}}(t) - \frac{H^{dr}_{\mathrm{TES}}(t)}{\eta_{dr}} \right) \cdot \Delta t \tag{2a}$$

$$Q^{\min}_{\mathrm{TES}} \le Q_{\mathrm{TES}}(t) \le Q^{\max}_{\mathrm{TES}} \tag{2b}$$

$$0 \le H^{\mathrm{in}}_{\mathrm{TES}}(t) \le \frac{1}{\eta_{\mathrm{in}}} \cdot H^{\max}_{\mathrm{in}} \tag{2c}$$

$$0 \le H^{dr}_{\mathrm{TES}}(t) \le \eta_{dr} \cdot H^{\max}_{dr} \tag{2d}$$

$$H^{\mathrm{in}}_{\mathrm{TES}}(t) \cdot H^{dr}_{\mathrm{TES}}(t) = 0, \text{ and } \begin{cases} H^{\mathrm{in}}_{\mathrm{TES}}(t) \ge 0 \\ H^{dr}_{\mathrm{TES}}(t) \ge 0. \end{cases} \tag{2e}$$

C. Electric Vehicles

Likewise, constraints for electric vehicles are set according to (3). Constraint (3a) represents the stored energy of the jth electric vehicle at time t. By (3b) and (3c), the charge and discharge will be kept within the capacity scope. Constraints (3d) and (3e) pose limits on the discharge and charge power. With (3f), the battery cannot charge and discharge simultaneously. In (3g), the upper and lower limits of capacity are considered

$$E_{\mathrm{EV},j}(t) = E_{\mathrm{EV},j}(t-1) + \eta_{ch,j} \cdot P^{ch}_{\mathrm{EV},j}(t) \cdot \Delta t - \frac{1}{\eta_{dch,j}} \cdot P^{dch}_{\mathrm{EV},j}(t) \cdot \Delta t \tag{3a}$$

$$0 \le \frac{1}{\eta_{dch,j}} \cdot P^{dch}_{\mathrm{EV},j}(t) \cdot \Delta t \le E_{\mathrm{EV},j}(t-1) \tag{3b}$$

$$0 \le \eta_{ch,j} \cdot P^{ch}_{\mathrm{EV},j}(t) \cdot \Delta t \le \mathrm{Cap}_{,j} - E_{\mathrm{EV},j}(t-1) \tag{3c}$$

$$0 \le P^{ch}_{\mathrm{EV},j}(t) \le P^{\max}_{ch,j} \tag{3d}$$

$$0 \le P^{dch}_{\mathrm{EV},j}(t) \le P^{\max}_{\mathrm{d}ch,j} \tag{3e}$$

$$P^{ch}_{\mathrm{EV},j}(t) \cdot P^{dch}_{\mathrm{EV},j}(t) = 0, \quad \text{and} \begin{cases} P^{ch}_{\mathrm{EV},j}(t) \ge 0 \\ P^{\mathrm{d}ch}_{\mathrm{EV},j}(t) \ge 0 \end{cases} \tag{3f}$$

$$E_{\mathrm{EV}_j}^{\min} \le E_{\mathrm{EV},j}(t) \le E_{\mathrm{EV}_j}^{\max}. \tag{3g}$$

D. Photovoltaic Power Generation System

The power output of the photovoltaic system is modeled as a deterministic model and expressed as [14], [23]

$$P_{\mathrm{PV}}(t) = \eta_{\mathrm{PV}} \cdot S \cdot I(t) \cdot [1 - 0.005 \cdot (T_{\mathrm{out}}(t) + 25)]. \tag{4}$$

E. Gas Boiler

The relationship between natural gas consumption and the heating output of the gas boiler is given in (5a). Ramping constraints are expressed in (5b). With (5c), the maximum and minimum output heating powers are considered

$$F_{\mathrm{GB}}(t) = \frac{H_{\mathrm{GB}}(t)}{\eta_{\mathrm{GB}}} \cdot \rho \cdot \Delta t \tag{5a}$$

$$-H^{d}_{\mathrm{GB}} \cdot \Delta t \le H_{\mathrm{GB}}(t) - H_{\mathrm{GB}}(t-1) \le H^{u}_{\mathrm{GB}} \cdot \Delta t \tag{5b}$$

$$H^{\min}_{\mathrm{GB}} \le H_{\mathrm{GB}}(t) \le H^{\max}_{\mathrm{GB}}. \tag{5c}$$

F. Electric Chiller

With the coefficient of performance, the cooling produced by the electric chiller is expressed in (6a). By (6b), the maximum and minimum output powers are considered

$$C_{\mathrm{EC}}(t) = P_{\mathrm{EC}}(t) \cdot \mathrm{cop}_{\mathrm{EC}} \tag{6a}$$

$$P_{\mathrm{EC}}^{\min} \le P_{\mathrm{EC}}(t) \le P_{\mathrm{EC}}^{\max}. \tag{6b}$$

G. Absorption Chiller

Similarly, the cooling generated by the absorption chiller is given in (7a). At the same time, the maximum and minimum output heating powers are considered by

$$C_{\mathrm{AC}}(t) = H_{\mathrm{AC}}(t) \cdot \mathrm{cop}_{\mathrm{AC}} \tag{7a}$$

$$H_{\mathrm{AC}}^{\min} \le H_{\mathrm{AC}}(t) \le H_{\mathrm{AC}}^{\max}. \tag{7b}$$

IV. Optimal Scheduling of IES With Multiple CCHPs

A. Objective Function

As stated in Section II-A, the second-order polynomial has an opening downward for GHG emissions, while for the power efficiency, the opening is downward. At the same time, the largest power efficiency and the lowest GHG emissions will not appear at the same load rate. Therefore, there is a conflict between the operation cost and GHG emissions. To find a solution to coordinate the operation cost and GHG emissions, a multiobjective optimal scheduling of IES with multiple CCHPs is proposed, as shown in

$$\min\left(F^{C}, F^{\mathrm{EM}}\right) \tag{8}$$

where

$$F^{C} = \sum_{t=1}^{T}\left(F_e^{P}(t) + F_g^{P}(t) - F_e^{S}(t) + F^{\mathrm{UD}}(t)\right) \tag{9}$$

$$F^{\mathrm{EM}} = \sum_{t=1}^{T} E_{\mathrm{total}}(t). \tag{10}$$

Equation (9) shows that the operation cost consists of the electricity cost, gas cost, electricity revenue, and startup/shutdown cost of CCHPs. The specific calculation is as follows:

$$\begin{aligned} F_e^{P}(t) &= P_e^{\mathrm{net}}(t) \cdot c_e(t) \cdot \Delta t \\ F_g^{P}(t) &= F_g^{\mathrm{net}}(t) \cdot c_g(t) \\ F_e^{S}(t) &= P_{\mathrm{out}}(t) \cdot \varsigma_e(t) \cdot \Delta t \\ F^{\mathrm{UD}}(t) &= \sum_{i=1}^{n}\sum_{t=1}^{T}\left(c_{cs,i} \cdot y_i(t) + c_{cd,i} \cdot z_i(t)\right). \end{aligned}$$

B. Energy Balance Constraints

According to Fig. 3, the electrical, thermal, cooling, natural gas, and emissions balances are given in

$$\begin{aligned} L_e(t) = {} & P_e^{\mathrm{net}}(t) + P_{\mathrm{PV}}(t) + \sum_{i=1}^{n} P_{\mathrm{CCHP},i}(t) + \sum_{j=1}^{m} P_{\mathrm{EV},j}^{dch}(t) \\ & - \sum_{j=1}^{m} P_{\mathrm{EV},j}^{ch}(t) - P_{\mathrm{EC}}(t) - P^{\mathrm{out}}(t) \end{aligned} \tag{11}$$

$$\begin{aligned} L_h(t) = {} & \sum_{i=1}^{n} H_{\mathrm{CCHP},i}(t) + H_{\mathrm{GB}}(t) \\ & + H_{\mathrm{TES}}^{dr}(t) - H_{\mathrm{TES}}^{\mathrm{in}}(t) - H_{\mathrm{AC}}(t) \end{aligned} \tag{12}$$

$$L_c(t) = C_{\mathrm{EC}}(t) + C_{\mathrm{AC}}(t) \tag{13}$$

$$F_g^{P}(t) = F_{\mathrm{GB}}(t) + \sum_{i=1}^{n} F_{\mathrm{CCHP},i}(t) \tag{14}$$

$$E_{\mathrm{total}}(t) = P_e^{\mathrm{net}}(t) \cdot \mu_{pc} \cdot \Delta t + F_{\mathrm{GB}}(t) \cdot \mu_{gc} + \sum_{i=1}^{n} E_{\mathrm{CCHP},i}(t). \tag{15}$$

C. Multiple Energy Exchanged Constraints

The power exchange between EH and the power grid is restricted by (16a) and (16b). Meanwhile, constraint (16c) ensures that purchasing and selling of electricity do not exist simultaneously. The gas transmission between EH and the natural gas network is limited as (17)

$$0 \le P_e^{\mathrm{net}}(t) \le P_{\mathrm{net}}^{\max} \tag{16a}$$

$$0 \le P^{\mathrm{out}}(t) \le P_{\mathrm{out}}^{\max} \tag{16b}$$

$$P_e^{\mathrm{net}}(t) \cdot P^{\mathrm{out}}(t) = 0 \tag{16c}$$

$$0 \le F_g^{\mathrm{net}}(t) \le F_{\mathrm{net}}^{\max}. \tag{17}$$

Therefore, while considering (1)–(17), the multiobjective optimal scheduling of the IES with multiple CCHPs as a MINLP problem is proposed to minimize both operation cost and GHG emissions. To solve the proposed MINLP model, the DICOPT solver under GAMS is used, which is widely used due to its ability to quickly solve nonconvex problems and match the best algorithms to the problem [36].

V. Proposed NLP Model and Solution

A. Fast Unit Commitment Technique

The proposed MINLP model as a NP-hard problem is difficult to be solved high efficiently. To improve the computational efficiency, a fast unit commitment technique [28] is used to transform the proposed MINLP model into a NLP one by approximating the rigorous unit commitment constraints. The fast unit commitment method mainly includes two steps: 1) the units with similar operation characteristics are aggregated as a group and 2) continuous variables which are used to describe different groups are introduced to approximate commitment decisions. Every CCHP is here considered as a group due to small-scale CCHPs. As a result, the continue variable (i.e., the online capacity), which is used to describe a group, can determine the on/off of individual CCHP. In other words, while the online capacity of the ith CCHP is equal to 0, the ith CCHP is off, and vice versa.

According to the rigorous unit commitment constraints in (1e)–(1g), the aggregated behaviors of CCHPs can be described as

$$\widehat{S}_k^{O}(t) = \sum_{i=1}^{K}\left(v_i(t) \cdot P_{\mathrm{CCHP},i}^{\max}\right) \tag{18}$$

$$\widehat{S}_k^U(t) = \sum_{i=1}^{K} \left(y_i(t) \cdot P_{\mathrm{CCHP},i}^{\max}\right) \tag{19}$$

$$\widehat{S}_k^D(t) = \sum_{i=1}^{K} \left(z_i(t) \cdot P_{\mathrm{CCHP},i}^{\max}\right) \tag{20}$$

where K indicates the number of CCHPs within the group. $\widehat{S}_k^O(t)$ is the online capacity, defined as the sum of the capacities of the kth group CCHPs that are operating at time t; $\widehat{S}_k^U(t)$ is the startup capacity, defined as the sum of the capacities of the kth group startup CCHPs at time t; $\widehat{S}_k^D(t)$ is the shutdown capacity, defined as the sum of the capacities of the kth group shut down CCHPs at time t.

As shown in (18), $\widehat{S}_k^O(t)$ determined by the binary variable $v_i(t)$, which leads to the discrete solution and decreases the computational efficiency. Therefore, $\widehat{S}_k^O(t)$ is relaxed as a continuous variable $S_k^O(t)$ shown in

$$0 \le S_k^O(t) \le S_k^I. \tag{21}$$

Similarly, $\widehat{S}_k^U(t)$ and $\widehat{S}_k^D(t)$ are expressed as

$$0 \le S_k^U(t), S_k^D(t) \le S_k^I. \tag{22}$$

In (21) and (22), S_k^I represents the total capacity of the kth group CCHPs, which is defined as

$$S_k^I = \sum_{i=1}^{I} P_{\mathrm{CCHP},i}^{\max}. \tag{23}$$

According to (1e), three continuous variables in (21) and (22) satisfy the following expression:

$$S_k^O(t) - S_k^U(t) = S_k^O(t-1) - S_k^D(t). \tag{24}$$

In this case, a total of $3 \times K$ binary variables, which define the on/off, startup, and shutdown status of CCHPs in group k, are replaced by three continuous variables identifying the online, startup, and shutdown capacities. This approach not only transforms the mixed-integer problem into a computationally efficient continuous problem but also significantly reduces the number of decision variables.

Therefore, based on the continuous variable defined in (21) and (22), the maximum and minimum limits of the power output of the kth group CCHPs at time t are expressed as

$$\underline{A}_k \cdot S_k^O(t) \le P_k(t) \le \overline{A}_k \cdot S_k^O(t) \tag{25a}$$

where $\overline{A}_k$ and $\underline{A}_k$ denote the ratios of maximum and minimum power output with respect to the capacity for the kth group CCHP and satisfy

$$\begin{cases} \overline{A}_k = \sum_{i=1}^{I} \left(\overline{\alpha}_i \cdot P_{\mathrm{CCHP},i}^{\max}\right)/S_I \\ \underline{A}_k = \sum_{i=1}^{I} \left(\underline{\alpha}_i \cdot P_{\mathrm{CCHP},i}^{\max}\right)/S_I. \end{cases} \tag{25b}$$

In (25b), $\overline{a}_i$ and $\underline{a}_i$ are the ratios of minimum and maximum power outputs with respect to its nameplate capacity for the ith CCHP in the kth group.

Then, with (21)–(25), the (1h) is reformulated as

$$\begin{cases} P_k(t) - P_k(t-1) \le (\underline{A}_k(t) \cdot S_k^U(t) - \underline{A}_k(t) \cdot S_k^D(t) \\ \quad + R_k^u(S_k^O(t) - S_k^U(t) - S_k^D(t+1))) \cdot \Delta t \\ P_k(t) - P_k(t-1) \ge (\underline{A}_k(t) \cdot S_k^U(t) - \underline{A}_k(t) \cdot \ S_k^D(t) \\ \quad - R_k^d(S_k^O(t) - S_k^U(t) - S_k^U(t-1))) \cdot \Delta t \end{cases} \tag{26}$$

where R_k^u and R_k^d, respectively, represent the ratios of the upward and downward ramping power to the online capacity for the kth CCHPs group, which are calculated similarly to the procedure specified in (25b).

For the minimum online/offline constraints, applying the three continuous variables described in (21) and (22), constraints (1g) and (1h) are reformulated in

$$\begin{cases} 0 \le S_k^D(1) \le S_k^O(0) \\ 0 \le S_k^D(t+1) \le S_k^O(t) - \sum_{\tau=0}^{t-1} S_k^U(t-\tau),\ 1 \le t \le \mathrm{UT}-1 \\ 0 \le S_k^D(t+1) \le S_k^O(t) - \sum_{\tau=0}^{\mathrm{UT}-2} S_k^U(t-\tau),\ \mathrm{UT} \le t \le T-1 \end{cases} \tag{27a}$$

$$\begin{cases} 0 \le S_k^U(1) \le S_I - S_k^O(0) \\ 0 \le S_k^U(t+1) \le S_I - S_k^O(t) - \sum_{\tau=0}^{t-1} S_k^D(t-\tau),\ 1 \le t \le \mathrm{DT}-1 \\ 0 \le S_k^U(t+1) \le S_I - S_k^O(t) - \sum_{\tau=0}^{\mathrm{DT}-2} S_k^D(t-\tau),\ \mathrm{DT} \le t \le T-1 \end{cases} \tag{27b}$$

where $S_k^O(0)$ is the online capacity of the kth group CCHPs at the initial time, and T is the number of time intervals.

Finally, the efficiency and emission of CCHPs are expressed with (28) and (29), and the startup and shutdown cost functions are represented in

$$\eta_k(t) = A_k + B_k \cdot P_k(t) + C_k \cdot {P_k}^2(t) \tag{28}$$

$$E_k(t) = \alpha_k + \beta_k \cdot P_k(t) + \gamma_k \cdot P_k^2(t) \tag{29}$$

$$F_k^{\mathrm{UD}}(t) = C_k^U \cdot S_k^U(t) + C_k^D \cdot S_k^D(t) \tag{30}$$

where A_k, B_k, and C_k are the equivalent efficiency coefficients; α_k, β_k, and γ_k are the equivalent emission coefficients; and C_k^U and C_k^D define fuel costs per unit startup and shutdown capacities, respectively.

Therefore, the MINLP model proposed in Section IV is transformed into a NLP model with the objective (8) and constraints (1c)–(1d), (2)–(7), and (9)–(30). The CONOPT solver based on the generalized reduced gradient algorithm in GAMS is used to solve the proposed NLP model, as it can deal with the large-scale nonlinear optimization [36]. When the largest component of the reduced gradient is less than the tolerance with default value 1.e-7, the best solution will be found.

B. Multiobjective to Single Objective Transformation

As the ε-constraint method can efficiently obtain the Pareto optimal solution set without the requirement of a unified scale and provide a representative subset of the Pareto set which in most cases is adequate [37], it is here used to solve the proposed multiobjective optimal problem. Although this method has been proposed for many years, it is effective in dealing with the multiobjective optimization problem and has been extensively used [23], [34], [38], [39]. According to this method, the number of the Pareto optimal solution can be adjusted by the number of grid points in each one of the objective functions. While using the fuzzy satisfying

method [23], [40]–[42], the best compromise solution from the Pareto optimal solution set can be obtained. The procedure is described in detail, as follows.

Step 1: Find the maximum and minimum of the cost function (9) and the emission function (10).

Step 2: Divide the range of the emissions objective functions into p equal intervals. Therefore, there are in total $(p+1)$ grid points and the value of the lth point is as

$$\varepsilon_l = F^{\mathrm{EM}}_{\max} - \frac{F^{\mathrm{EM}}_{\max} - F^{\mathrm{EM}}_{\min}}{p} \cdot l, \quad l = 0, 1, \ldots, p.$$

Step 3: Add the emissions objective function to the constraint in the lth calculation as

$$F^{\mathrm{EM}} \leq \varepsilon_l$$

Step 4: Minimize F^C to obtain Pareto-optimal solution by (31) and form the Pareto optimal solution set

$$\min F^C \quad \text{subjected to}: \begin{cases} F^{\mathrm{EM}} \leq \varepsilon_l \\ \text{constraints (1c)}-\text{(1d)}, \text{ (2)}-\text{(7)}, \text{ and (9)}-\text{(30)}. \end{cases} \tag{31}$$

Step 5: Define the following membership functions to choose the best solution from Pareto optimal solution set:

$$\mu^{F_p(X_l)} = \begin{cases} 0, & \text{otherwise} \\ \frac{F_p^{\max} - F_p(X_l)}{F_p^{\max} - F_p^{\min}}, & F_p^{\min} \leq F_p(X_l) \leq F_p^{\max} \end{cases} \tag{32}$$

where $F_p^{\max}$ and $F_p^{\min}$ are the maximum and minimum values in the Pareto optimal front for the pth objective function. $F_p(X_l)$ and $\mu^{F_p(X_l)}$ are the value of the lth solution in the Pareto optimal front for the pth objective function and its corresponding membership function, respectively. The value of $\mu^{F_p(X_j)}$ varies between 0 to 1 and shows the success degree of $F_p(X_j)$ in minimizing the objective function p.

Step 6: Find the best solution based on the membership functions as

$$\max_{l=1:n} \left(\min_{p=1:2} \mu^{F_p(X_l)} \right). \tag{33}$$

C. Solution Algorithm

According to the above solution, the algorithm shown in Algorithm 1 is used to perform the optimal dispatch.

Algorithm 1 Optimal Dispatch of the Proposed EH

a. Initialization: Input EH parameters such as initial values (e.g. U_i^0, S_i^0), maximum and minimum of each subsystem (e.g.,$Q_{TES}^{\max}/Q_{TES}^{\min}$, $P_{GT,i}^{\max}/P_{GT,i}^{\min}$), ramping rate (e.g., $P_{GT,i}^{u}/P_{GT,i}^{d}$).

Main procedure:

b. Update state parameters such as demands and prices at t (e.g., $L_e(t)$, $c_g(t)$), states at $t-1$ (e.g. $P_{CCHP,i}(t-1)$, $P_{GB}(t-1)$).

c. Solve the scheduling model (6) subjected to (1c) -(1d), (2)–(7), and (9)–(30) by following steps.

Step 1: Find the maximum and minimum of the cost function (9) and emission function (10).

Step 2: Divide the range of the emissions objective functions into l equal intervals.

Step 3: Add the emission objective to the constraints.

Step 4: Minimize cost function (9) to obtain the Pareto optimal solution set according to (31).

d. Choose the best solution from Pareto optimal solution set by the following steps.

Step 1: Define membership functions for OF^C and OF^{EM} according to (32).

Step 2: Find the best solution according to (33).

e. Send the optimal dispatch such as$P_e^{net}(t)$, $P_{EV}^{ch}(t)$, $P_{GT}(t)$, $P_{EC}(t)$, $P_{AC}(t)$ to each subsystem.

f. Time $T+1$, return to step b.

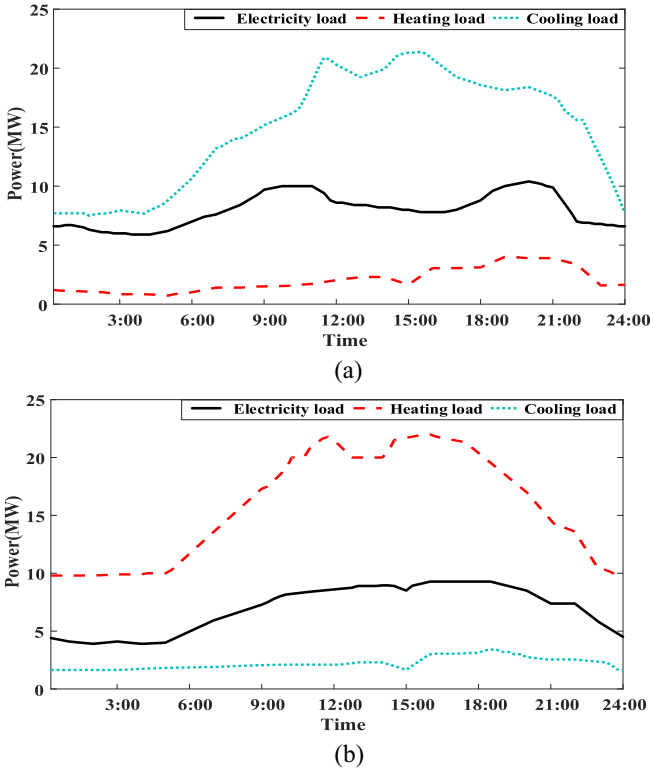

Fig. 4. Cooling, heating, and electricity loads on typical days. (a) On a typical summer day. (b) On a typical winter day.

VI. Simulations and Results

A. System Parameters

The architecture of the IES is shown in Fig. 1. The cooling, heating, and electricity loads on typical days are illustrated in Fig. 4. The time-of-use prices of electricity, gas, and selling electricity are given in Table II [14]. While using the time-series model [43], the forecasted solar radiation is shown in Fig. 5. We assumed that the departure and arrival times of EVs are, respectively, 8:00 A.M. and 17:00 P.M., and their initial and arrival battery SoC levels obey normal distributions simulated by the Monte Carlo method. The parameters of EVs, the emission factor of the electricity from the grid, the cooling coefficient of electric chiller, the cooling coefficient of adsorption chiller, etc., are given in Table III [14], [23]. Three CCHPs are here considered, and the relevant parameters are shown in Table IV [32], [44]. Note that for three CCHPs, CCHP1 has the minimal capacity, while CCHP3 has the maximal capacity.

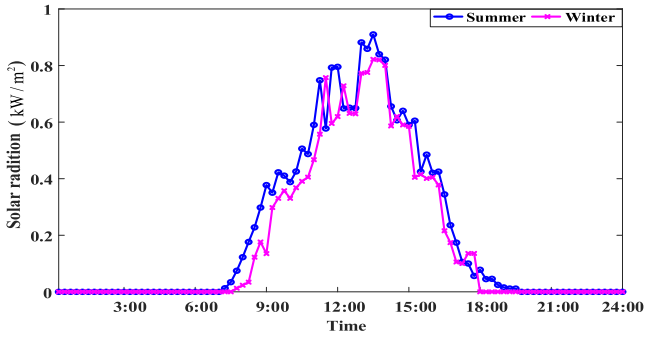

Fig. 5. Forecasted solar radiation using the time-series model.

TABLE II
TIME-OF-USE ELECTRICITY PRICE, GAS PRICE, AND SELLING TARIFF

Time	Electricity $c_e(t)$ (¥/kWh)	Gas $c_g(t)$ (¥/m^3)	Revenue $\varsigma_e(t)$ (¥/kWh)
7:00-10:00	0.678	2.73	0.691
10:00-16:00	1.009	2.73	1.024
16:00-18:00	0.678	2.73	0.691
18:00-22:00	1.009	2.73	1.024
22:00-7:00	0.356	2.73	0.356

TABLE III
PARAMETERS OF OTHER SUBSYSTEMS IN IES

Parameters	Value	Parameters	Value
The number of EVs	600	μ_{pc} / μ_{gc}	968/220
Departure/arrival times	8:00 a.m. /17:00 p.m.	cop_{EC} / cop_{AC}	4/1.2
Capacity	27.4	$H_{GB}^{\max}$ / $H_{GB}^{\min}$	0/4
$P_{ch,j}^{\max}$ / $P_{dch,j}^{\max}$	3.6/2.9	H_{GB}^{u} / H_{GB}^{d}	0.2/0.2
$\eta_{ch,j}$ / $\eta_{dch,j}$	0.92/0.92	$H_{AC}^{\max}$ / $H_{AC}^{\min}$	5/0
$SOC_{0,j}$	$SOC_0 \sim N(0.3, 0.01)$	$P_{EC}^{\max}$ / $P_{EC}^{\min}$	4.5/0
$SOC_{re,j}$	$SOC_{re} \sim N(0.3, 0.01)$	$P_{net}^{\max}$ / $P_{out}^{\max}$	10/10
		$F_{net}^{\max}$	1000

B. Results and Discussions

To validate the effectiveness of the proposed MINLP and NLP model, comparisons among MINLP, NLP, and the IES with a single CCHP (IES-SC) are conducted on summer and winter scenarios.

1) Total Operation Cost and GHG Emissions: As shown in Table V, both summer and winter days, the operation cost and GHG emissions of MINLP are lower than those of IES-SC. As multiple CCHPs can be coordinated to improve the energy efficiency according to MINLP, the natural gas and electricity purchased from external networks are lower. This results in significantly lower gas and electricity costs in both summer and winter compared with IES-SC. On the other hand, by MINLP, the less natural gas results in less GHG emissions generated by CCHPs in summer and winter, compared with IES-SC. As a result, the total operation cost and GHG emissions of MINLP are lower than those of IES-SC, although there are some differences in start-up/shut-down costs, revenue for the electricity sale, and emissions from the gas boiler and network electricity. Therefore, considering multiple CCHPs in the optimal scheduling of IES has better advantages over a single CCHP in improving energy efficiency and reducing GHG emissions.

TABLE IV
PARAMETERS OF CCHP SYSTEMS IN MINLP/NLP AND IES-SC

Symbol	Quantity	MINLP/NLP			IES-SC
		CCHP1	CCHP2	CCHP3	S-CCHP
C_{cs} / C_{cd}	Start-up / shut-down cost	56.6	62.3	78.2	-
P^u / P^d	Ramping up/down rate	0.09	0.12	0.18	0.39
S^{I}	Capacity	3	4	6	13
$P_{\max}$ / $P_{\min}$	Maximum/minimum power	3/0.3	4/0.4	6/0.6	13/1.3
η_W	WHB efficiency	0.8	0.8	0.8	0.8
a	First efficiency coefficient	0.27	0.255	0.228	0.193
b (10^{-2})	Second efficiency coefficient	7.33	7.28	6.24	3.77
c (10^{-2})	Third efficiency coefficient	-1.67	-1.32	-0.75	-0.21
α	First emission coefficient	69.3	76.5	83.3	244.5
β	Second emission coefficient	-37.5	-35.5	-29.2	-37.6
γ	Third emission coefficient	12.1	8.4	4.6	2.72

As shown in Table V, the total operation cost of NLP does not increase significantly compared with that of MINLP, in both summer and winter. This is because although the electricity cost is higher, the gas and start-up/shut-down costs are lower on a summer day. On a winter day, the difference of the electricity cost, gas cost, and the revenue for electricity is slight in MINLP and NLP, while the startup/shutdown costs are the same. Regarding GHG emissions, the total GHG emissions of NLP are slightly higher, because NLP has higher GHG emissions from CCHPs and network electricity than MINLP does on a summer day. However, on a winter day, NLP has basically the same GHG emissions as MINLP, because of the slightly different GHG emissions from CCHPs, the gas boiler, and the network electricity. Note that the total operation cost and GHG emissions in both cases are lower than those of IES-SC. On the other hand, as shown in Table VI, the computational speed for NLP is 4.01-times faster than MINLP on a summer day. Similarly, 3.86-times improvement in computational speed for the winter case between NLP and MINLP can be found. Therefore, the fast unit commitment method can improve the computational efficiency of IES with multiple CCHPs, while ensuring calculation accuracy.

2) Overall Power Efficiency and GHG Emissions of CCHPs: To compare the power efficiency of IES-SC, MINLP, and NLP, we here define the overall power efficiency of CCHPs in the IES

$$\eta_{\text{all}}(t) = \frac{\sum_{i=1}^{n} \left(\eta_{e,i}(t) \cdot P_{\text{CCHP},i}(t)\right)}{\sum_{i=1}^{n} P_{\text{CCHP},i}(t)}.$$

Compared with S-CCHP in IES-SC, the overall power efficiency of CCHPs in MINLP on a summer day is always higher and the GHG emissions are lower, as shown in Fig. 6. This is because CCHPs in MINLP are combined to follow load changes by optimally committing CCHPs, as illustrated in Fig. 7. In detail, CCHP2 works during 0:00–1:15 and 22:45-24:00; following the change of load, CCHP1 works from 1:15 to 6:30, CCHP3 works between 6:45 to 9:30; to satisfy the increase of electricity and cooling load, CCHP1 and CCHP2 work together about 9:30-12:45; while CCHP3 run to meet the demand during 12:45-22:45. On the contrary, S-CCHP with

TABLE V
COMPARISONS OF COSTS AND EMISSIONS OF IES-SC, MINLP, AND NLP

Results	Summer			Winter		
	IES-SC	MINLP	NLP	IES-SC	MINLP	NLP
Electricity Cost (¥)	105839.9	101644.2	102829.5	113.9	29.9	22.9
Gas cost (¥)	69905.6	65223.5	64730.8	190484.9	189590.5	189574.8
Start-up/shut-down cost (¥)	0	788.4	337	0	113.2	113.2
Revenue for the electricity sale (¥)	0	0	0	74541.9	73891.7	73862.5
Total costs (¥)	**175745.5**	**167656.1**	**167897.3**	**116056.9**	**115841.9**	**115848.4**
Emissions from CCHP (kg)	14771.3	6185.2	7646.3	16509.1	15119.5	15189.0
Emissions from GB (kg)	0	0	0	36.6	100.2	100.2
Emissions from network electricity (kg)	155947.5	157108.2	158715.7	309.8	81.4	62.2
Total emissions (kg)	**170718.8**	**163293.4**	**166362.0**	**16855.5**	**15301.1**	**15351.4**

TABLE VI
COMPUTATIONAL TIME OF MINLP AND NLP

	computational Time(s)		Times
	MINLP	NLP	
Summer	9959	2485	4.01
Winter	7121	1844	3.86

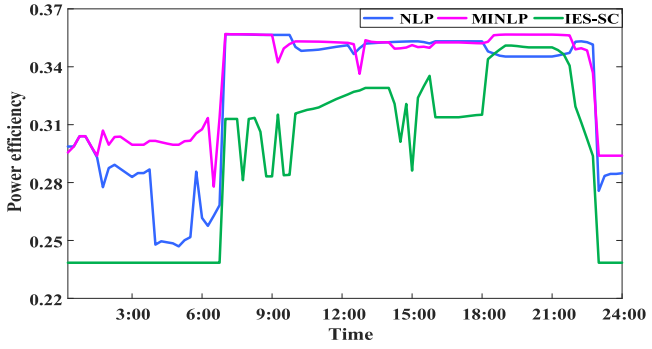

(a)

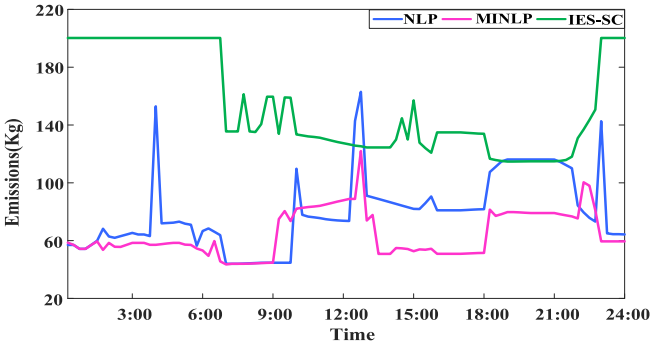

(b)

Fig. 6. (a) Overall power efficiency and (b) GHG emissions of CCHPs on a summer day.

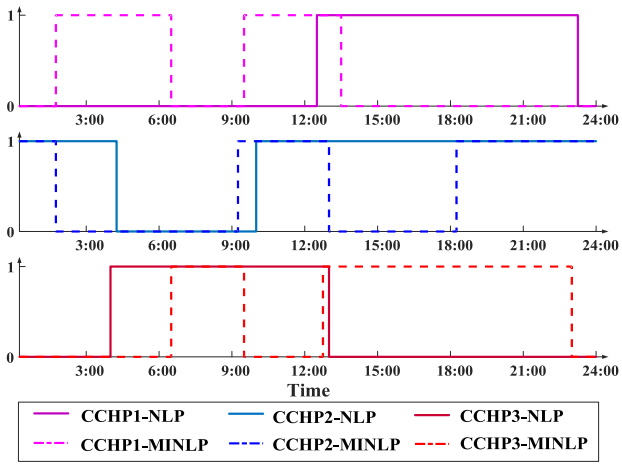

Fig. 7. Unit commitment of CCHPs on a summer day.

the large capacity in IES-SC always runs with lower power efficiency and higher GHG emissions due to the small demand.

Compared with MINLP, NLP has the lower overall power efficiency and the higher GHG emissions during 0:15-6:30 and 22:45-24:00, as shown in Fig. 6. This is because NLP is approximated based on the online capacity, leading to the combination of CCHPs in NLP being different from that in MINLP, as illustrated in Fig. 7. For instance, during 1:15-6:30, CCHP1 in MINLP works, while for NLP, CCHP2 and CCHP3, respectively, work during 1:15-4:30 and 4:30-6:30. This will result in a slight difference in overall power efficiency and GHG emissions between NLP and MINLP, as shown in Fig. 6. In other periods, the difference is smaller even equal to 0. Therefore, although NLP has some loss of accuracy compared with MINLP, the loss is very small. In summary, the overall power efficiency and GHG emissions of CCHPs in NLP and MINLP are not significantly different and are better than those of IES-SC.

On a winter day, the overall power efficiency of CCHPs for MINLP is higher than that of S-CCHP in IES-SC, except for about 6: 00 or 22: 00, as shown in Fig. 8. The GHG emissions of MINLP are lower on the whole day. This is because CCHPs in MINLP are coordinated to match load levels with high efficiency and low-GHG emissions shown in Fig. 8. For instance, around 0:00–6:00 and 22:45-24:00, CCHP2 and CCHP3 work together to maintain higher efficiency and lower GHG emissions. Then, as the loads increase, three CCHPs in MINLP operate. For IES-SC, although S-CCHP with a large capacity works at a high-load rate, high-load rate does not mean low-operation cost and GHG emissions, as demonstrated in Section II-A.

As for MINLP and NLP, the differences in overall power efficiency and GHG emissions of CCHPs are quite small, as shown in Fig. 8. The discrepancies are mainly attributed to the approximation of ramping constraints. As shown in Fig. 8, CCHP1 of MINLP starts at 6:15 and stops at 22:45, while CCHP1 of NLP starts at 6:30 and stops at 22:30. This will

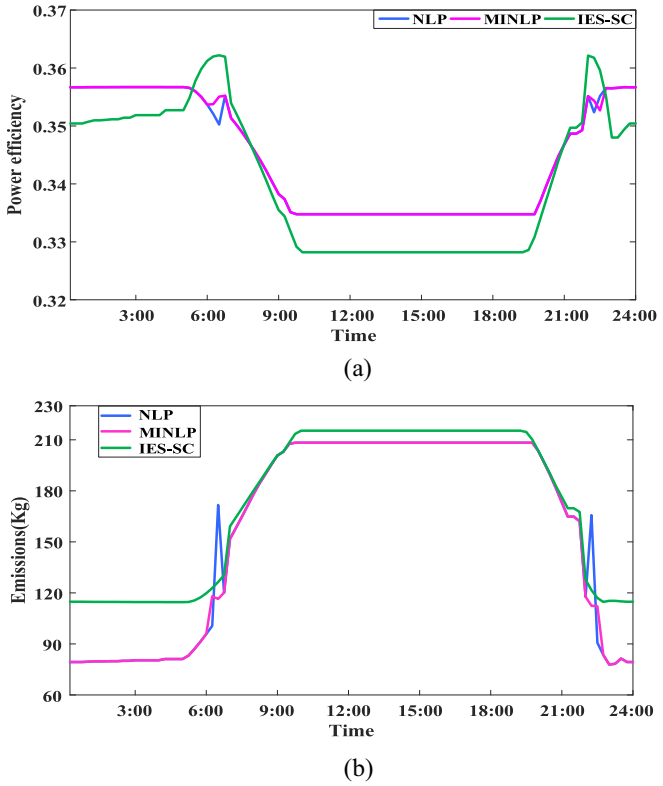

Fig. 8. (a) Overall power efficiency and (b) GHG emissions of CCHPs on a winter day.

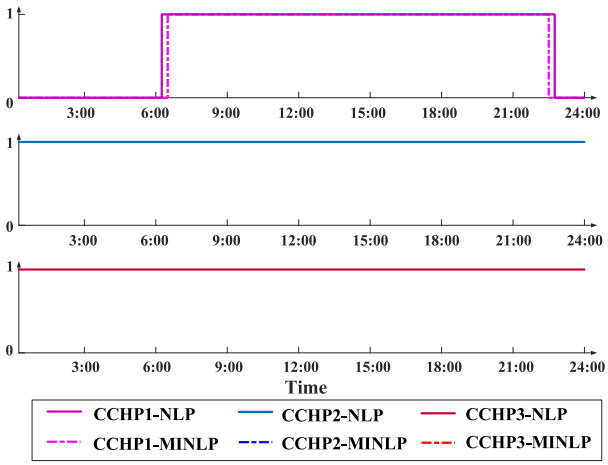

Fig. 9. Unit commitment of CCHPs on a winter day.

result in a slightly higher overall power efficiency of CCHP and slightly lower GHG emissions, compared with NLP.

In summary, the proposed MINLP can improve energy efficiency and reduce GHG emissions, compared with IES-SC, whether in winter or summer. Moreover, the proposed NLP can maintain the computational accuracy and improve the computational efficiency compared with MINLP.

3) Coordination of Multiple Energy Flows: To clarify the coordination of multienergy flows in the IESs by committing multiple CCHPs, we take the time window of 1:00–10:00 on a summer day as an example, as illustrated in Figs. 10 and 11.

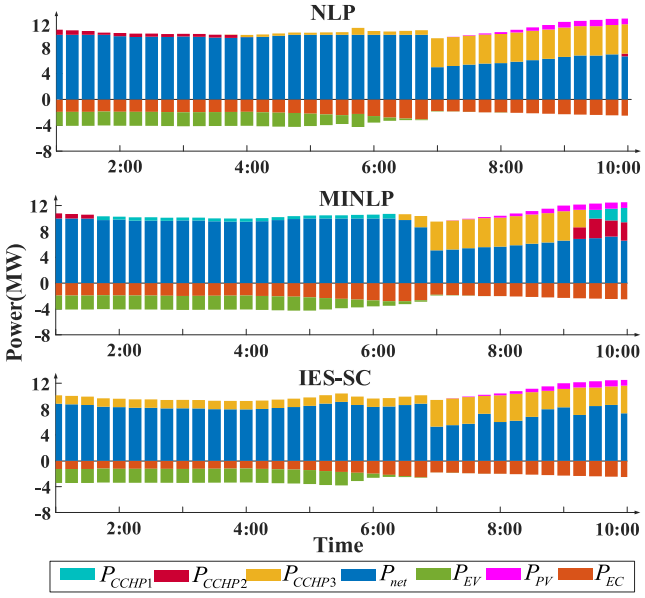

Fig. 10. Power outputs of IESs on a summer day.

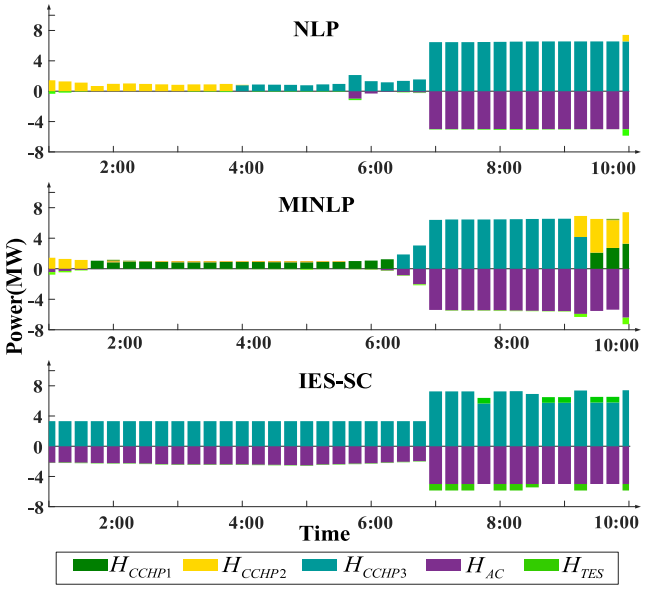

Fig. 11. Heating outputs of IESs on a summer day.

During 1:00–7:00, both on IES-SC, MINLP, and NLP, IESs buy a lot of electricity from the power grid due to the electricity price being off-peak, as shown in Fig. 10. Currently, CCHPs operate at the minimum operating point. From 7:00 to 10:00, with electricity price and loads increasing, the electricity purchased from the grid decreases and the electricity generated by CCHPs increases. At these times, the electricity is used for electricity demand, charging of electric vehicles, and cooling demand. The heating generated by CCHPs is used to meet heating demand and for refrigeration, as shown in Fig. 11.

For MINLP and NLP, different unit commitments of CCHPs affected by the approximation of start-up and shut-down costs can be observed, but total outputs of CCHPs are the same, as shown in Fig. 10. Therefore, the outputs of other subsystems in

NLP are the same as those of MINLP. The comparison further confirms the effectiveness of NLP in the optimal scheduling of IES.

However, total outputs of CCHPs are different for IES-SC and MINLP or NLP, as shown in Fig. 10. For example, between 1:00–7:00, the output of CCHP in MINLP or NLP is less than S-CCHP, which results in more electricity purchased from the power grid. Nonetheless, the operation cost of MINLP or NLP is less than IES-SC, because the electricity price is off-peak. Furthermore, due to the lower power efficiency and higher GHG emissions at the minimum output of large-capacity S-CCHP, the operation cost and GHG emissions of IES-SC are higher. To sum up, IES can coordinate multi-energy flow by multi-CCHP commitments to reduce operation cost and GHG emissions.

VII. Conclusion

In this article, an optimal EH model is proposed to minimize operation cost and GHG emissions considering multiple CCHPs with different capacities. With the constraints, such as the unit commitment of CCHPs and the nonlinear couplings between the power efficiency and GHG emissions of CCHP and its load rate, the proposed multiobjective problem is constructed as a MINLP model. To improve the computational efficiency, the proposed MINLP model is transformed into a NLP one by the fast unit commitment method. Simulation results show that compared with IES with a single CCHP, the proposed MINLP and NLP can effectively reduce the operation cost and GHG emissions; in particular, the proposed NLP has a faster computational speed while keeping a high-computational accuracy in comparison to the proposed MINLP.

The commitment operation of multiple CCHPs can not only improve the economy and environmental-friendliness of IES but also improve the flexibility of IES, which is helpful in ensuring the normal operation of IES in some serious cases like strong uncertainties. Therefore, our future work will focus on the optimal operation of multiple CCHPs in these cases.

References

[1] T. Ding, W. Jia, M. Shahidehpour, O. Han, Y. Sun, and Z. Zhang, "Review of optimization methods for energy hub planning, operation, trading, and control," *IEEE Trans. Sustain. Energy*, vol. 13, no. 3, pp. 1802–1818, Jul. 2022.

[2] X. Jin, Q. Wu, H. Jia, and N. D. Hatziargyriou, "Optimal integration of building heating loads in integrated heating/electricity community energy systems: A bi-level MPC approach," *IEEE Trans. Sustain. Energy*, vol. 12, no. 3, pp. 1741–1754, Jul. 2021.

[3] S. Zhang, W. Gu, S. Yao, S. Lu, S. Zhou, and Z. Wu, "Partitional decoupling method for fast calculation of energy flow in a large-scale heat and electricity integrated energy system," *IEEE Trans. Sustain. Energy*, vol. 12, no. 1, pp. 501–513, Jan. 2021.

[4] L. Gan-Yun, C. Bin, J. De-Xiang, W. Nan, L. Jun, and C. Guangyu, "Optimal scheduling of regional integrated energy system considering integrated demand response," *CSEE J. Power Energy Syst.*, early access, Sep. 10, 2021, doi: 10.17775/CSEEJPES.2020.06160

[5] C. Y. Zheng, J. Y. Wu, and X. Q. Zhai, "A novel operation strategy for CCHP systems based on minimum distance," *Appl. Energy*, vol. 128, pp. 325–335, Sep. 2014.

[6] R. Hashemi, "A developed offline model for optimal operation of combined heating and cooling and power systems," *IEEE Trans. Energy Convers.*, vol. 24, no. 1, pp. 222–229, Mar. 2009.

[7] D. Arthur. "Cooling, heating, and power (CHP) for commercial buildings benefits analysis." Aug. 2008. [Online]. Available: http://www.eere.energy.gov/de/chp/chp_applications/information_resources.html>

[8] N. Fumo, P. J. Mago, and L. M. Chamra, "Emission operational strategy for combined cooling, heating, and power systems," *Appl. Energy*, vol. 86, no. 11, pp. 2344–2350, Nov. 2009.

[9] H. Cho, P. J. Mago, R. Luck, and L. M. Chamra, "Evaluation of CCHP systems performance based on operational cost, primary energy consumption, and carbon dioxide emission by utilizing an optimal operation scheme," *Appl. Energy*, vol. 86, no. 12, pp. 2540–2549, Dec. 2009.

[10] M. Hu and H. Cho, "A probability constrained multi-objective optimization model for CCHP system operation decision support," *Appl. Energy*, vol. 116, no. 116, pp. 230–242, Mar. 2014.

[11] F. Fang, Q. H. Wang, and Y. Shi, "A novel optimal operational strategy for the CCHP system based on two operating modes," *IEEE Trans. Power Syst.*, vol. 27, no. 2, pp. 1032–1041, May 2012.

[12] P. Favre-Perrod, "A vision of future energy networks," in *Proc. IEEE Power Eng. Society Inaugural Conf. Expo. Africa*, Jul. 2006, pp. 13–17.

[13] T. Ha, Y. Zhang, V. V. Thang, and J. Huang, "Energy hub modeling to minimize residential energy costs considering solar energy and BESS," *J. Mod. Power Syst. Clean Energy*, vol. 5, no. 3, pp. 389–399, May 2017.

[14] H. Yang, T. Xiong, and J. Qiu, "Optimal operation of DES/CCHP based regional multi-energy prosumer with demand response," *Appl. Energy*, vol. 167, pp. 353–365, Apr. 2016.

[15] A. Heidari, "Stochastic effects of ice storage on improvement of an energy hub optimal operation including demand response and renewable energies," *Appl. Energy*, vol. 261, pp. 114393–114404, Mar. 2020.

[16] J. Hu, X. Liu, M. Shahidehpour, and S. Xia, "Optimal operation of energy hubs with large-scale distributed energy resources for distribution network congestion management," *IEEE Trans. Sustain. Energy*, vol. 12, no. 3, pp. 1755–1765, Jul. 2021.

[17] M. S. Javadi, M. Lotfi, A. E. Nezhad, A. Anvari-Moghaddam, J. M. Guerrero, and J. P. S. Catalão, "Optimal operation of energy hubs considering uncertainties and different time resolutions," *IEEE Trans. Ind. Appl.*, vol. 56, no. 5, pp. 5543–5552, Sep./Oct. 2020.

[18] T. Liu, D. Zhang, H. Dai, and T. Wu, "Intelligent modeling and optimization for smart energy hub," *IEEE Trans. Ind. Electron.*, vol. 66, no. 12, pp. 9898–9908, Dec. 2019.

[19] C. Zhang, Y. Xu, Z. Li, and Z. Y. Dong, "Robustly coordinated operation of a multi-energy microgrid with flexible electric and thermal loads," *IEEE Trans. Smart Grid*, vol. 10, no. 3, pp. 2765–2775, May 2019.

[20] T. Ma, J. Wu, and L. Hao, "Energy flow modeling and optimal operation analysis of the micro energy grid based on energy hub," *Energy Convers. Manag.*, vol. 133, pp. 292–306, Feb. 2017.

[21] T. Ha, Y. Xue, K. Lin, Y. Zhang, V. Van Thang, and T. Nguyen, "Optimal operation of energy hub based micro-energy network with integration of renewables and energy storages," *J. Mod. Power Syst. Clean Energy*, vol. 10, no. 1, pp. 100–108, Jan. 2022.

[22] Y. Luo, X. Zhang, D. Yang, and Q. Sun, "Emission trading based optimal scheduling strategy of energy hub with energy storage and integrated electric vehicles," *J. Mod. Power Syst. Clean Energy*, vol. 8, no. 2, pp. 267–275, Mar. 2020.

[23] F. Brahman, M. Honarmand, and S. Jadid, "Optimal electrical and thermal energy management of a residential energy hub, integrating demand response and energy storage system," *Energy Build.*, vol. 90, pp. 65–75, Mar. 2015.

[24] G. Li et al., "Optimal dispatch strategy for integrated energy systems with CCHP and wind power," *Appl. Energy*, vol. 192, pp. 408–419, Apr. 2017.

[25] G. Li, R. Zhang, T. Jiang, H. Chen, L. Bai, and X. Li, "Security-constrained bi-level economic dispatch model for integrated natural gas and electricity systems considering wind power and power-to-gas process," *Appl. Energy*, vol. 194, pp. 696–704, May 2017.

[26] Y. Jiang et al., "Coordinated operation of gas-electricity integrated distribution system with multi-CCHP and distributed renewable energy sources," *Appl. Energy*, vol. 211, pp. 237–248, Feb. 2018.

[27] G. E. Alvareza, M. G. Marcovecchio, and P. A. Aguirre, "Security-constrained unit commitment problem including thermal and pumped storage units: A MILP formulation by the application of linear approximations techniques," *Electr. Power Syst. Res.*, vol. 154, pp. 67–74, Jan. 2018.

[28] X. Han, X. Chen, M. B. Mcelroy, S. Liao, C. P. Nielsen, and J. Wen, "Modeling formulation and validation for accelerated simulation and flexibility assessment on large scale power systems under higher renewable penetrations," *Appl. Energy*, vol. 237, pp. 145–154, Mar. 2019.

[29] A. Canova, G. Chicco, G. Genon, and P. Mancarella, "Emission characterization and evaluation of natural gas-fueled cogeneration microturbines and internal combustion engines," *Energy Convers. Manag.*, vol. 49, no. 10, pp. 2900–2909, Oct. 2008.
[30] S. Bando, H. Watanabe, H. Asano, and S. Tsujita, "Impact of various characteristics of electricity and heat demand on the optimal configuration of a microgrid," *Electr. Eng. Japan*, vol. 169, no. 2, pp. 6–13, 2009.
[31] M. Liu, Y. Shi, and F. Fang, "A new operation strategy for CCHP systems with hybrid chillers," *Appl. Energy*, vol. 95, pp. 164–173, Jul. 2012.
[32] L. Li, H. Mu, and W. Gao, "Optimization and analysis of CCHP system based on energy loads coupling of residential and office buildings," *Appl. Energy*, vol. 136, pp. 206–216. Dec. 2014.
[33] V. Vahidinasab and S. Jadid. "Joint economic and emission dispatch in energy markets: A multi-objective mathematical programming approach," *Energy*, vol. 35, no. 3, pp. 1497–1504. Mar. 2010.
[34] H. Falsafi, A. Zakariazadeh, and S. Jadid, "The role of demand response in single and multi-objective wind-thermal generation scheduling: A stochastic programming," *Energy*, vol. 64, no. 1, pp. 853–886. Jan. 2014.
[35] J. Wang, Y. Sun, R. Mahfound, H. H. Alhelou, and P. Siano, "Integrated modeling of regional and park-level multi-heterogeneous energy systems," *Energy Rep.*, vol. 8, pp. 3141–3155, Nov. 2022.
[36] A. Brook, D. Kendrick, and A. Meeraus, "GAMS: A user's guide," *ACM SIGNUM Newslett.*, vol. 23, nos. 3–4, pp. 10–11, 1988.
[37] G. Mavrotas, "Effective implementation of the ε-constraint method in multi-objective mathematical programming problems," *Appl. Math. Comput.*, vol. 213, no. 2, pp. 455–465, Jul. 2009.
[38] Y. Cao, Q. Wang, J. Du, S. Nojavan, K. Jermsittiparsert, and N. Ghadimi, "Optimal operation of CCHP and renewable generation-based energy hub considering environmental perspective: An Epsilon constraint and fuzzy methods," *Sustain. Energy, Grids Netw.*, vol. 20, Dec. 2019, Art. no. 100274.
[39] L. He and L. Zhang, "A bi-objective optimization of energy consumption and investment cost for public building envelope design based on the ε-constraint method," *Energy Build.*, vol. 266, Jul. 2022, Art. no. 112133.
[40] A. Soroudi and M. Afrasiab, "Binary PSO-based dynamic multi-objective model for distributed generation planning under uncertainty," *IET Renew. Power Gener.*, vol. 6, no. 2, pp. 67–78, 2012.
[41] R. Gholizadeh-Roshanagh, K. Zare, and M. Marzband, "An a-posteriori multi-objective optimization method for MILP-based distribution expansion planning," *IEEE Access*, vol. 8, pp. 60279–60292, 2020.
[42] S. Zeynali, N. Rostami, and M. R. Feyzi, "Multi-objective optimal short-term planning of renewable distributed generations and capacitor banks in power system considering different uncertainties including plug-in electric vehicles," *Int. J. Electr. Power*, vol. 119, Jul. 2020, Art. no. 105885.
[43] J. W. Taylor, P. E. McSharry, and R. Buizza, "Wind power density forecasting using ensemble predictions and time series model," *IEEE Trans Energy Convers.*, vol. 24, no. 3, pp. 775–782, Sep. 2009.
[44] A. Rong and R. Lahdelma, "An effective heuristic for combined heat-and-power production planning with power ramp constraints," *Appl. Energy*, vol. 84, no. 3, pp. 307–325, Mar. 2007.

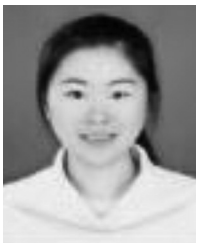

Haimin Xie received the B.S. degree in electrical engineering from Xi'an University of Technology, Xi'an, China, in 2017. She is currently pursuing the Ph.D. degree with the College of Electrical Engineering, Guangxi University, Nanning, China.

Her current research interests include integrated energy systems and auxiliary service for frequency regulation and demand response.

Hui Liu (Senior Member, IEEE) received the M.S. and Ph.D. degrees in electrical engineering from the College of Electrical Engineering, Guangxi University, Nanning, China, in 2004 and 2007, respectively.

He worked with Tsinghua University, Beijing, China, as a Postdoctoral Fellow from 2011 to 2013 and in Jiangsu University, Zhenjiang, China, as a Faculty Member from 2007 to 2016. He visited the Energy Systems Division with Argonne National Laboratory, Lemont, IL, USA, from 2014 to 2015. He joined the School of Electrical Engineering, Guangxi University in 2016, where he is a Professor and a Deputy Dean.

Prof. Liu is an Editor of the IEEE TRANSACTIONS ON SMART GRID and the IEEE Power Electronics Letters. He is also an Associate Editor of the *IET Smart Grid* and the *IET Generation, Transmission and Distribution*. His research interests include power system optimization, power system stability and control, electric vehicles, integrated energy systems, and demand response.

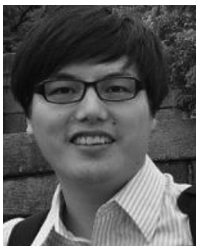

Can Wan (Senior Member, IEEE) received the B.Eng. degree from Zhejiang University, Hangzhou, China, in 2008, and the Ph.D. degree from The Hong Kong Polytechnic University, Hong Kong, in 2015.

He is currently a Professor with the College of Electrical Engineering, Zhejiang University. He was a Postdoctoral Fellow with the Department of Electrical Engineering, Tsinghua University, Beijing, China, and held a research positions with the Technical University of Denmark, Kongens Lyngby, Denmark; The Hong Kong Polytechnic University; and The City University of Hong Kong, Hong Kong. He was a Visiting Scholar with the Center for Electric Power and Energy, Technical University of Denmark, and Argonne National Laboratory, Lemont, IL, USA. His research interests include forecasting, power system uncertainty analysis and control, renewable energy integration, and machine learning.

Hui Hwang Goh (Senior Member, IEEE) received the B.Eng. degree (Hons.) in electrical engineering, the M.Eng. degree in electrical engineering, and the Ph.D. degree from the Universiti Teknologi Malaysia, Skudai, Malaysia, in 1998, 2002, and 2007, respectively.

He is currently a Professor of Electrical Engineering, Guangxi University, Nanning, China. His research interests include embedded power generation modeling and simulation, power quality studies, multicriteria decision making, and high-voltage technique.

Dr. Goh is a Fellow of the Institution of Engineering and Technology, Stevenage, U.K. He is also a Fellow of the Chinese Society of Electrical Engineering, and a Chartered Engineer under the Engineering Council United Kingdom.

Saifur Rahman (Life Fellow, IEEE) received the B.Sc. degree in electrical engineering from Bangladesh University of Engineering and Technology, Dhaka, Bangladesh, in 1973, the M.S. degree in electrical engineering from the State University of New York, New York, NY, USA, in 1975, and the Ph.D. degree in electrical engineering from Virginia Tech, Blacksburg, VA, USA, in 1978.

He is currently the Founding Director of the Advanced Research Institute, Virginia Tech, Arlington, VA, USA, where he is also the J. R. Loring Professor of Electrical and Computer Engineering. He also directs the Center for Energy and the Global Environment, Virginia Tech. He has lectured on renewable energy, energy efficiency, smart grid, energy Internet, blockchain, and IoT sensor integration in over 30 countries.

Prof. Rahman is an IEEE Millennium Medal Winner. He was the Founding Editor-in-Chief of *IEEE Electrification Magazine* and the IEEE TRANSACTIONS ON SUSTAINABLE ENERGY. He has served as the Chair of the U.S. National Science Foundation Advisory Committee for International Science and Engineering from 2010 to 2013. He was the President of the IEEE Power and Energy Society for 2018 and 2019 and a 2022 IEEE President-Elect. He is also a Distinguished Lecturer for PES.